Performance limits of electrical cables for intrasystem communication

by A. Deutsch

G. Arjavalingam

C. W. Surovic

A. P. Lanzetta

K. E. Fogel

F. Doanv

M. B. Ritter

Three types of cables (commercially available high-performance coaxial and ribbon cables. and an experimental flexible-film cable) were investigated for intrasystem communication in high-performance computer and communication systems. The electrical properties of the cables and their respective connectors were obtained and compared through the use of time-domain techniques. Feasibility for use in digital signal propagation at 500 Mb/s-1 Gb/s was demonstrated by means of pulse propagation and eye-diagram measurements. Performance limits in terms of maximum useful cable lengths were determined through simulations which included the effects of associated connectors, vias, and printed-circuit-card wiring.

Introduction

Cables will be required for intrasystem communication in forthcoming high-performance multiprocessor computers, in which individual processors are expected to function at clock rates of several hundred MHz. Similar needs are anticipated for forthcoming communication systems, which will have to carry digital signals at Gb/s data rates. In this

study, we have investigated relevant performance limits of the following types of electrical cables and their respective connectors: commercially available high-performance coaxial and ribbon cables, and an experimental flexible-film cable. The signal-propagation characteristics of the cables were studied through propagation measurements with a 2-ns-wide pulse. Associated bit-error-rate and eye-diagram measurements were conducted with a pseudorandom sequence of pulses at different clock rates to ascertain the performance limits of the three types of cables. The measured parameters were then used in detailed simulations to provide guidelines for maximum useful lengths of the cables in intrasystem interconnections.

The paper is organized as follows. First, the measured values of the electrical attenuation, phase constant, and impedance properties of the cables up to 8 GHz are described and compared with specifications provided by the cable manufacturers. Then, the determination of the capacitive and inductive discontinuities introduced by the cable connectors using 20- and 70-GHz sampling oscilloscopes are described. Also described is the crosstalk generated in the connectors and in the vias connecting the cables to transmission lines in associated printed-circuit cards. Finally, measurements pertaining to the propagation of representative 2-ns-wide pulses are described.

Copyright 1994 by International Business Machines Corporation. Copying in printed form for private use is permitted without payment of royalty provided that (1) each reproduction is done without alteration and (2) the Journal reference and IBM copyright notice are included on the first page. The title and abstract, but no other portions, of this paper may be copied or distributed royalty free without further permission by computer-based and other information-service systems. Permission to republish any other portion of this paper must be obtained from the Editor.

Table 1 Characteristics of cables investigated in this study. (ϵ_r = dielectric constant of insulator, τ = propagation delay per unit length, R = resistance per unit length, Z_0 = characteristic impedance, ATT = attenuation at 1 GHz, t_r = rise time observed at end of cable.)

(Cable type	τ (ps/cm)	R (Ω/cm)	$Z_0 \atop (\Omega)$	ATT @ 1 GHz (dB/cm)	t _r (ps)
Coaxial 25AWG (18-mil diameter)	Expanded PTFE $\varepsilon_r = 1.3$ Braided ground conductor	39	0.00127	50	0.0136	353 @ 2 m
Ribbon (10-mil diameter)	Thermoplastic elastomer $\varepsilon_{\rm r} = 2.2$ Pleated-copper foil shield	50	0.004	53	0.02	536 @ 2 m
Flexible-film (5.5 × 1.4 mil)	Kapton $\varepsilon_r = 3.13$ Solid ground planes	59	0.033	45	0.06	434 @ 0.5 m

Cable characteristics

Although many variations of the coaxial, ribbon, and flexible-film cables were characterized, emphasis was placed primarily on three types because of their potential for satisfying anticipated increases in data transmission rates while also providing dense connectivity. The three cable types are listed in **Table 1** and depicted in **Figure 1**. Coaxial and ribbon cables are available from several manufacturers, including, for example, W. L. Gore & Associates, Inc., 3M's Electronic Product Division, and AMP Inc.

Typically, the cabling that will be required must be 1.5–5 m in length inside a single electronic enclosure, with connectors providing contact to associated card or board wiring at a 10–20-per-inch linear density. Up to several hundred cables, for example, might have to be attached to each printed-circuit card. Since constraints of space will force the cables to be bundled, we chose to investigate only well-shielded cables (necessary in order to avoid loss of energy through radiation, to maintain controlled impedance, and to minimize intra-cable crosstalk).

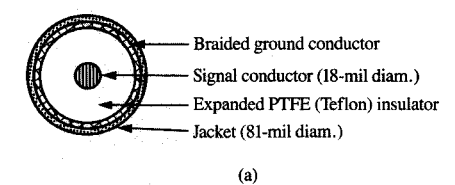
Coaxial cables are composed of a central conductor surrounded by a concentric conducting shell and designated by their military nomenclature, "RG-xy." They are available at different levels of quality. Some are suitable for use at bandwidths of 40 GHz. Such relatively high-performance cables contain thick shields and largediameter signal conductors in order to minimize resistive losses and signal distortion caused by attenuation and risetime dispersion, and require the use of relatively large connectors. Our investigations of coaxial cables were confined to a type having a relatively small diameter: the "improved" RG-type cable, which has an outer diameter of 2.057 mm (81 mils) and is available with a variety of inner conductor diameters. That type of cable has a braided outer ground conductor and an expanded (microporous) PTFE (Teflon®) insulator, as indicated in Figure 1(a). The cable can be attached to printed-circuit

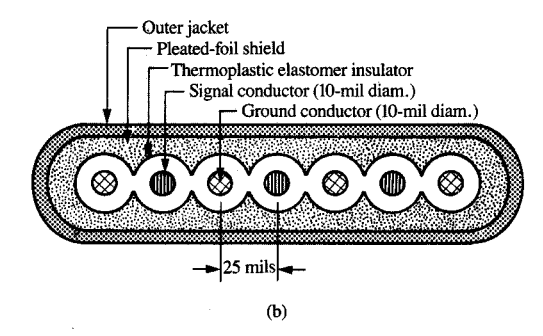
cards using either straight or 90° connectors with a matching header mounted on the card itself. The coaxial cables investigated were primarily those containing a 0.457-mm (18-mil)-diameter signal conductor, designated as a "gauge 25AWG" conductor.

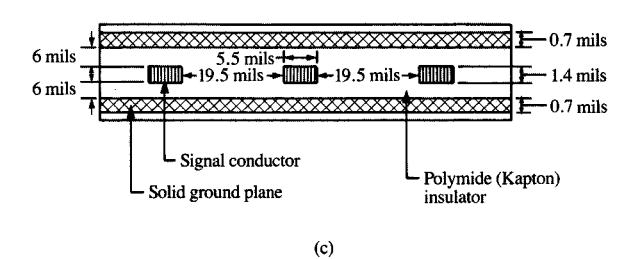
Among the other types of coaxial cables that are commercially available, some contain a thermoplastic-elastomer or foamed-polypropylene insulator; their ground conductor can be a thin foil with an inside drain wire that wraps spirally along the length of the cable. Cables of such a configuration have a nonuniform cross section, resulting in large variations in their electrical characteristics; they were found to have characteristics less suitable for high-performance applications than the braided type and are not discussed further.

The ribbon cable that was investigated contains 0.254-mm (10-mil)-diameter copper wires with 0.38-mm (15-mil) separations [Figure 1(b)] in a repetitive ground-signal-ground coplanar design. Its insulator is a thermoplastic elastomer. A thin pleated copper foil surrounds the cable to provide shielding, and is grounded in its connector by two contacts. The third type of cable investigated, a flexible-film cable, has a triplate structure, as shown in Figure 1(c). It contains 0.14-mm (5.5-mil)-wide, 0.036-mm (1.4-mil)-thick copper lines that are sandwiched between 0.018-mm (0.7-mil)-thick upper and lower reference planes, and a polyimide (Kapton®) insulator. The signal lines are separated by 0.635-mm (25-mil) center-to-center spacings, and the pads at the ends of the lines fan out to 1.27-mm (50-mil) grids (Figure 2).

The characteristic impedance Z_0 of all the cables investigated was close to 50 Ω . The choice of Z_0 depends on the overall system design. Lower Z_0 values generally result in lower crosstalk, higher density, and smaller reflections caused by discontinuities along the signal paths [1]. The use of thinner insulator layers leads to lower Z_0 ; however, the highest density is obtained if the signal conductors are scaled as well. Smaller cross sections result





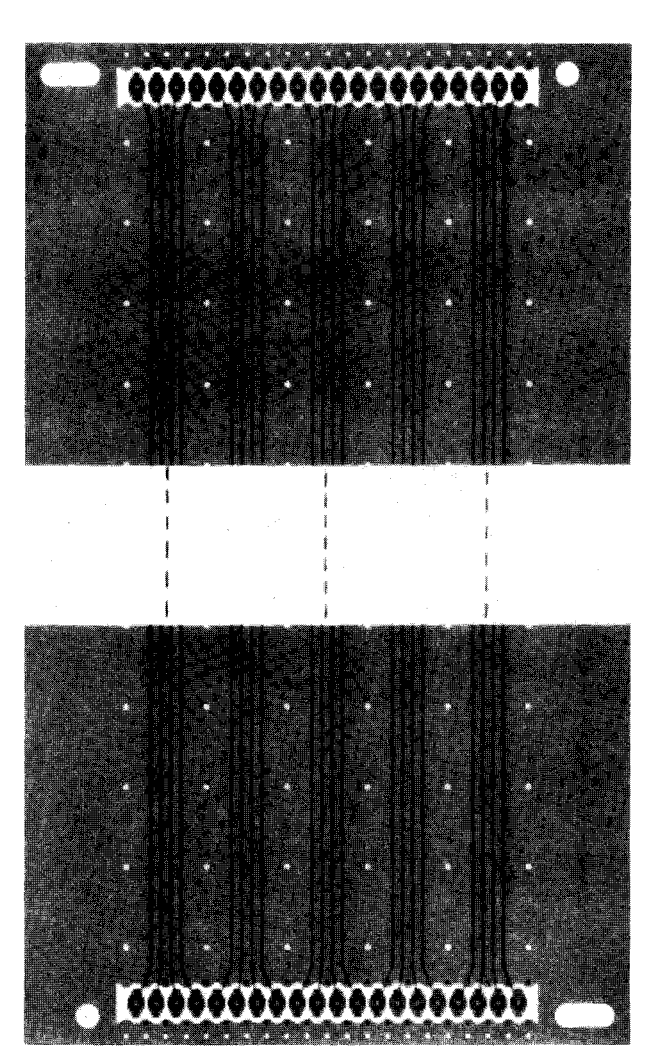


Schematic cross sections of cables investigated: (a) coaxial 25AWG cable, (b) ribbon cable, and (c) flexible-film cable.

in higher resistive losses, which in turn distort the signals. Also, the driver circuits would need to provide larger currents to charge the low-impedance lines, resulting in higher power dissipation.

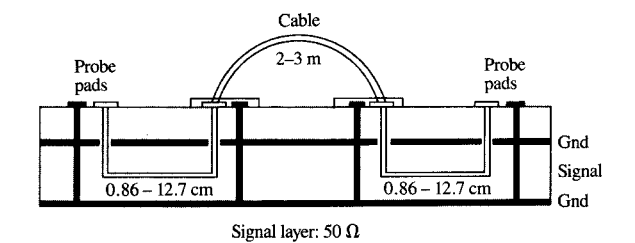
Cable investigations

The electrical properties of the cables were investigated first. For this purpose, test cards having the cross section shown in **Figure 3** were designed. The cards were fabricated with lines 0.406 mm (16 mils) wide and 0.035 mm (1.4 mils) thick, sandwiched between two ground planes. The wiring was designed to have a $50-\Omega$ characteristic impedance, and the line-to-line spacing was 50 mils. Signals were launched into the card trace with custom-made probes [2]. The signal then traveled a length of card trace and entered the connector through a via. The signal propagated on the cable and, at the output, was



an trak

Top view of flexible-film cable, showing signal and ground connector pads at the ends.



Cross section of test card having one signal layer between two ground planes.

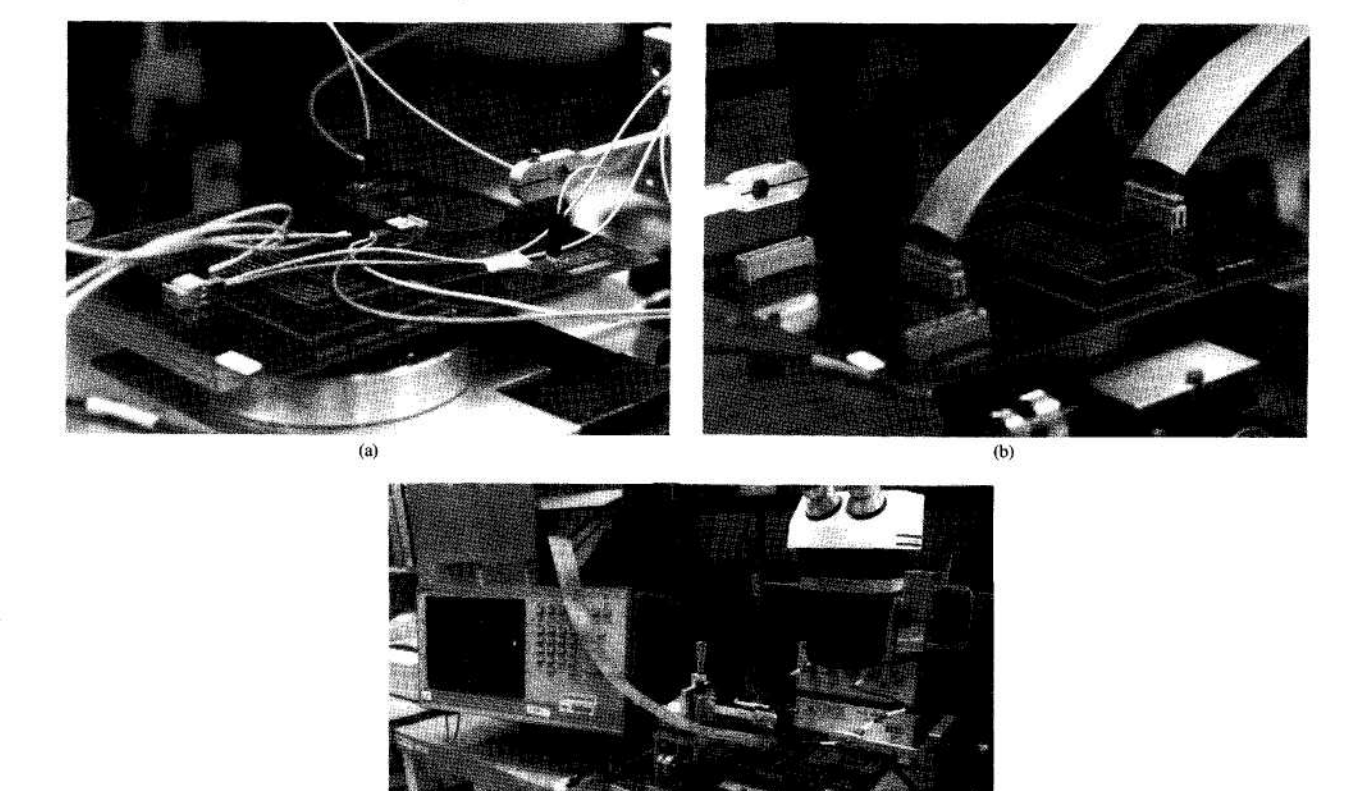


Figure 4

Close-up views during time-domain measurements, showing (a) coaxial 25AWG cable, (b) ribbon cable, and (c) flexible-film cable.

detected with another probe after passing through a second connector onto the card. Card traces 0.86 cm (0.34 in.) and 12.7 cm (5 in.) in length were used in order to evaluate the cable both with and without a representative card line. Each cable required a different card layout because of its unique connector footprint. The longer card wiring simulated typical applications in which the many driver circuits needed cannot be placed in close proximity to the cable ends.

Figure 4 shows the different cables investigated. Use was made of either an HP 54120A 20-GHz sampling oscilloscope or a Hypres PSP-1000 70-GHz picosecond signal processor. The measured waveforms were digitized, and signal analysis was performed by an IBM PS/2[®] computer. The short-pulse propagation technique described in [3] was used to obtain the attenuation, phase constant, and impedance, over a broad frequency range; these

parameters provide complete characterization of any transmission line. A 35-ps-wide pulse was created by an impulse-forming network (Picosecond Pulse Labs Model 5210) placed in line with the output step source of the 20-GHz sampling oscilloscope. The pulse was launched on two lengths of cables, 2 m and 3 m in the study of the coaxial and ribbon cables, and on lengths of 0.13 cm (very short) and 50 cm in the study of the flexible-film cable, as described in [3]. Because of the large discontinuities introduced by the cable connectors, the cables were first characterized without their connectors present. Since most of the attenuation data from cable manufacturers are only available up to 400 MHz, extrapolation based on skineffect losses was carried out in order to compare with our results up to 8 GHz. This could easily be done, since the attenuation increases with the square root of the frequency in the frequency range over which skin-effect losses are

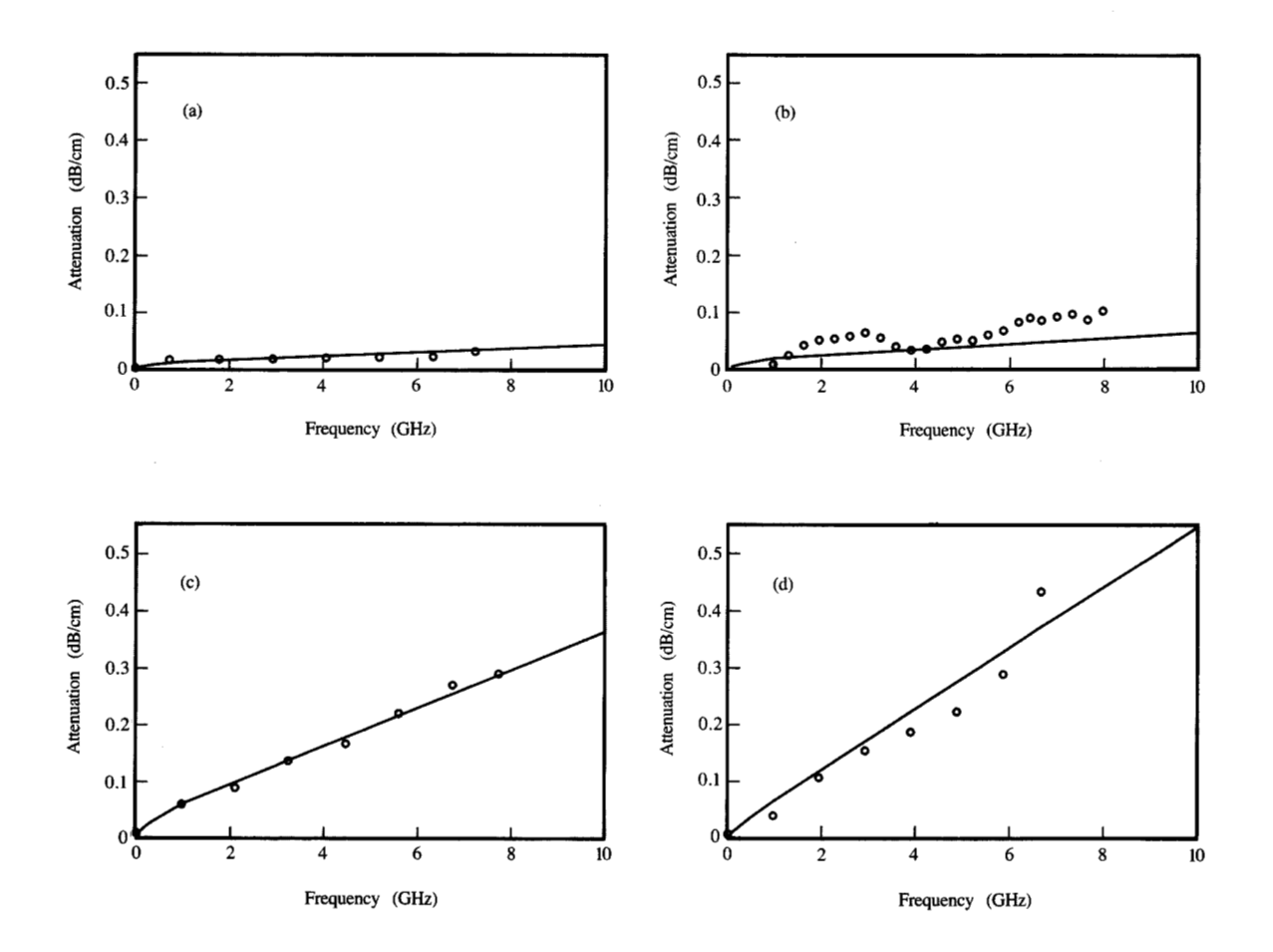


Figure 5

Measured (points) and manufacturer's data or calculated values (lines) for attenuation as a function of frequency for (a) coaxial 25AWG cable, (b) ribbon cable, (c) flexible-film cable, and (d) test card wiring.

dominant [1]. The results are shown in **Figure 5**. The cables had to be characterized up to these high frequencies, since transmission of signals at 0.5–1-Gb/s data rates requires the use of signals having rise times of 300–500 ps. Such transitions contain frequency components with significant energy up to 5–10 GHz.

The manufacturer's attenuation data for the ribbon cable imply greater losses than for the coaxial 25AWG cable; that was expected (and confirmed by measurement) because the ribbon cable contains 0.254-mm (10-mil)-diameter conductors, while the latter contains 18-mil-diameter signal lines. The attenuation for the ribbon cable was higher than predicted by skin-effect losses

alone—possibly because its thermoplastic elastomer exhibits significant dielectric loss above 1 GHz. Coaxial 30AWG cables (containing 10-mil-diameter conductors) were also characterized and found to exhibit losses similar to those of the ribbon cables. The measured frequency-dependent attenuation constant for the flexible-film cable is shown in Figure 5(c). As expected, its attenuation is much larger than the attenuation in the coaxial or ribbon cables because of its smaller conductor cross section $(0.14 \times 0.035 \, \text{mm})$. In fact, its attenuation is comparable to that of the card traces, which is shown in Figure 5(d). Table 1 includes the measured high-frequency characteristic impedances and the attenuation at 1 GHz for the coaxial, ribbon, and flexible-film cables. It should be noted that

even at 1 GHz, a 2-m coaxial 25AWG cable displays 2.72 dB of loss, which is not insignificant. The coaxial and ribbon cables display similar losses at 1 GHz, as seen in Figures 5(a) and 5(b), but the attenuation diverges at higher frequencies because of a combination of skin-effect and dielectric losses. The flexible-film cable displays the highest attenuation. It is not obvious from manufacturers' specifications (usually presented in the MHz frequency range) that such losses exist and that they limit extendability to GHz data rates. The short-pulse propagation technique described earlier can provide highfrequency characterization of such salient effects as dielectric loss, which become important at higher frequencies. At low frequencies, such losses are insignificant and are not apparent when measurements are performed in the subgigahertz frequency range.

Signal propagation delay, τl (where τ is the propagation delay per unit length, and l is the cable length) and rise time, t_{\cdot} , were measured with the test card of Figure 3. These are very important parameters for digital signal applications and directly affect the overall system performance. Table 1 summarizes the results obtained. As expected, τ was found to be smallest for the coaxial cable with expanded Teflon insulator, since it has the lowest dielectric constant ε_r (τ is proportional to $\sqrt{\varepsilon_r}/c$, where cis the velocity of light). Latency on these 2-m lengths of cables is not an important consideration for communication applications. Data streams are composed of large packets that occupy several-hundred-nanosecond (ns) time slots, while typical path delays are around 10 ns. Once the packet address is identified from the header data, the entire frame is synchronized. Since the header itself can be several tens of ns long, any synchronization requirement could be of the order of 1-5 ns, which is easily achieved because the cable propagation delay tolerances can be kept within $\pm 1-2\%$. What is most important in such cases is tight signal integrity control. By contrast, in applications such as memory access paths in tightly or even loosely coupled parallel processors, short propagation delays are important for overall system performance in addition to signal reliability and small timing jitter. The cables listed in Table 1 each displayed very tight delay tolerances and characteristic impedances close to 50 Ω . Although the flexible-film cable was designed to have that characteristic impedance, the subtractive copper etching used in its fabrication resulted in a trapezoidal cross section, with $Z_0 = 45 \ \Omega.$

Cable-connector investigations

The cables could be attached to cards with different types of connectors, providing the transition from their coaxial, coplanar-waveguide, or strip-line cable cross sections to those of the transmission lines in the printed-circuit boards. Use was made of either pinned or surface-to-

surface attachment to the vias in the cards. The space transformation from the uniform, high-density cable lines to the coarse vias and pads in the cards introduced significant signal distortion and crosstalk and had to be carefully evaluated.

The coaxial cables contained either individual 90° or straight-end-pinned connectors to the card (cable carrier), while the card connector (header) could be straight or have a 90° bend, as seen in Figure 4(a). The pin grid was 2.54 mm (0.1 in.). The header was either specially designed to match the cable impedance or consisted of simple 90° bent pins. In another instance, a two-row carrier connected to a header that fanned out to four rows of pins in the card. The ribbon cable was terminated with a two-row, grouped connector with pins on a 1.27 \times 2.54-mm (0.05 \times 0.1-in.) grid. The assignment of pins could be made such that alternate rows were grounded and used for signal transmission, or use could be made of a 45° staggered assignment in which alternating pins were used for signal transmission and were grounded, resulting in a 2.84-mm (0.112-in.) signal-to-signal pin separation. A metal shield, not shown, covered the connector and was contacted to the pleated-foil cable shield. Such a 40-pin connector, for example, yields only 18 signal contacts. The flexible-film cable was attached to the printed-circuit board with a novel surface-mount connector [4]. This connector could be made part of the cable or constructed on the card surface. In the former case, a raised hemispherical gold bump was plated on the end pads, as described in [5]. For our initial evaluation, the bumps were formed on the card surface. Gold wires were ball-bonded at an angle on the gold-plated card pads, and a laser was used to melt the wire into 0.254-mm (10-mil)-diameter ball contacts. A silicone elastomer which sets at room temperature was used to lock the wire bonds in place [4]. The flexible film, having a thin layer of "hard gold" on the end pads, was flipped face down and clamped to the card.

It was important to evaluate the capacitive and inductive discontinuities introduced by the cable connectors. If the cable-to-card interface delay is much smaller than the signal rise time t_r , the transition suffers minimal degradation. If the delay is close to $t_r/2$, the waveform is distorted and displays an increased rise time. Such discontinuities can generally be represented by lumped circuit elements. Inductive and capacitive discontinuities cause reflections which have amplitudes proportional to $[L/(2Z_0t_r)]\cdot V_{\rm in}$ or $(CZ_0/2t_r)\cdot V_{\rm in}$, respectively (where $V_{\rm in}$ is the input source signal) [1]. Such reflections can become significant if they are large enough to cause logic failure.

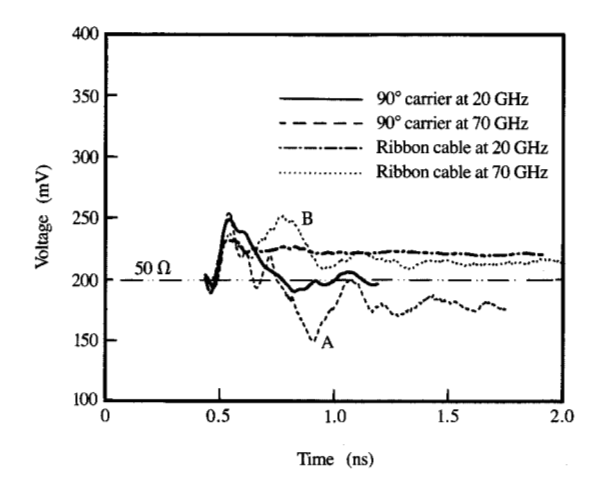
Time-domain reflectometry (TDR) measurements were performed to extract the effective discontinuities introduced by the various connectors. A voltage step was propagated down a transmission line which was attached to a connector, and the incident and reflected waves

were monitored at the oscilloscope input. Any impedance mismatch caused by the connectors was reflected back and thereby separated in time from the incident wave. The shape of the reflected wave reveals the nature and position of the discontinuity. A capacitive component results in a "dip," while an inductor generates a "peak" in the signal. This is due to the inability of the capacitor or inductor to respond to sudden changes in voltage or current, respectively. A fast voltage transition through a capacitor appears to indicate the presence of sudden "short circuit" on the line, with an equivalent low impedance which causes a negative spike in the voltage (a dip). Similarly, a fast current change through an inductor appears to indicate the presence of a high-impedance discontinuity, or an "open circuit," and hence a positive peak. Most connectors are characterized by a combination of both types of components.

Figure 6 shows the TDR results obtained using 20- and 70-GHz sampling oscilloscopes for the coaxial cable with the 90° carrier and for the ribbon cable connector. The results measured with a 15-ps rise-time source (PSP-1000 signal processor) showed additional capacitive components at point A (negative dip) for the 90° carrier and some inductive component at point B (positive peak) for the ribbon-cable connector that were not evident with the 20-GHz instrument, which only produces a 35-ps rise-time excitation. The peaks in the waveforms were fairly consistent, whichever instrument was used. The equivalent connector impedance, $Z_{\rm C}$ ($Z_{\rm C} = \sqrt{L/C}$) could be extracted from the reflection amplitude by using the relation [1]

$$Z_{\rm C} = Z_0 \frac{1 + \rho}{1 - \rho} \,, \tag{1}$$

where ρ is the reflection coefficient defined as $V_{\rm R}/V_{\rm in}$ and Z_0 is the impedance of the signal line attached to the connector. V_{p} is the amplitude of the dip or peak in the reflected waveform. The closest match to 50 Ω (which corresponds to the 200-mV level) was found with the 90° header for the coaxial cable and the surface-mount connector used with the flexible-film cable. While the very short rise times used in the measurements provide an accurate means of obtaining the connector models, representative logic signal transitions are much longer. In such cases, the amplitude of the reflections is significantly reduced. For instance, the 90° carrier for the coaxial cable displayed a peak equivalent to $Z_{\rm C}$ = 54 Ω when a rise time of 400 ps was used-an impedance which was much smaller than the 81 Ω measured with the 35-ps transition shown in Figure 6. This is one reason why, in practical applications for propagating 500-Mb/s data rates, the conventional approaches discussed in this study are still viable.

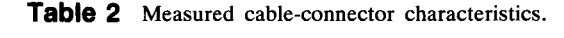


Time-domain reflectometry response of connector discontinuity for 90° carrier (solid and dashed lines) and ribbon-cable connectors (dot-dashed and dotted line), using 20- and 70-GHz oscilloscopes with 35- and 15-ps rise-time sources, respectively.

The criterion for signal integrity ensures that adequate signal amplitude propagates from the driver to the receiver circuit. The signal at the receiver circuit input must be larger than the total noise generated along the path, including crosstalk, simultaneously switching noise (ΔI) , and reflections. In most system designs, the receiver noise budget assumes about 10-15% (of the signal swing) for crosstalk allocation and about 10-15% for ΔI allocation. Typical printed-circuit-board traces generate crosstalk of the order of 7-10% of the driver output swing. Cables and cable connectors therefore should not introduce more than 3-5% of crosstalk. In all cases, the crosstalk in the cables investigated was found to be insignificant or nonexistent. Most discrete cables are well isolated by design. In general, crosstalk is generated by transfer of energy from active lines (carrying signals) to quiet adjacent lines through capacitive and inductive coupling, as explained in [6]. The capacitive and inductive components add at the driving end and subtract at the far end of the line. The near-end noise (NEN), monitored at the driving end, travels in the opposite direction from the active pulse and has a width equal to twice the line delay. The far-end noise (FEN) travels in the same direction as the active pulse and has a width equal to the rise time.

Crosstalk was measured with the test card of Figure 3 using a 300-ps rise-time step excitation similar to a representative driver-circuit output. We first measured the coupled noise in the 0.86-cm (0.34-in.) length of card trace





Connectors	$Z_0 \ (\Omega)$	<i>NEN</i> (%)	FEN (%)
Matched 90° carrier	81	2.6	2.86
Matched 90° header	61	3	3.5
Pinned ribbon	69	5	7
Surface-mount	58	3.5	3.5

The smallest crosstalk, observed with the 90° carrier, was 2.6 and 2.86% of the signal swing for the *NEN* and *FEN*, respectively. A straight cable carrier with a 90° header exhibited good impedance matching and only slightly higher crosstalk. The connector for ribbon cables displayed more crosstalk. This was reduced from 10% to 5% and from 10% to 7%, respectively, when the pin assignment was changed from one row of signal, one row of reference pins, to a staggered arrangement in which the signal-to-

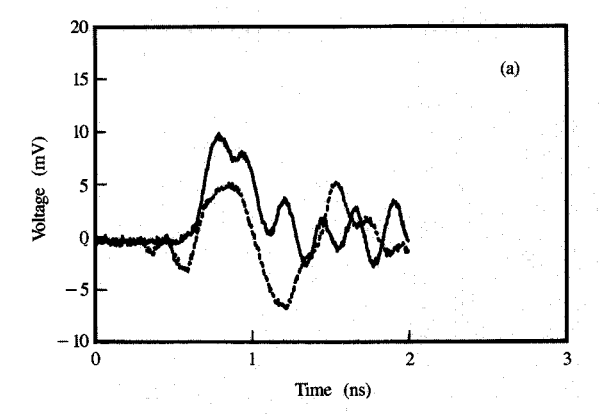
signal spacing increased from 1.27 mm to 2.84 mm (50 mils

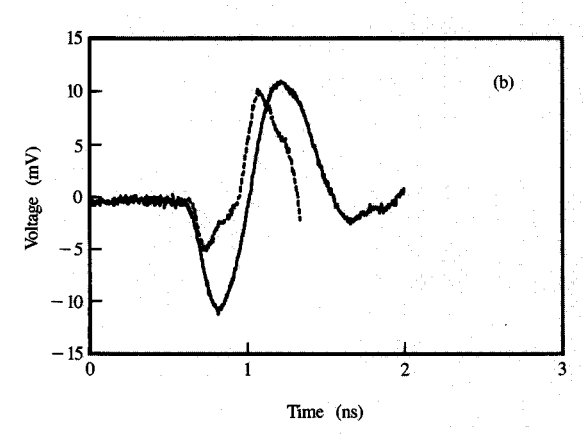
Pulse response

to 112 mils).

It was shown in Figure 5 that cable attenuation can become significant, especially for the long lengths of interest. The different frequency components contained in the rise time of digital signals attenuate differently and are shifted in phase differently. This effect results in rise-time degradation or dispersion [1]. Skin-effect and dielectric losses affect the higher frequencies the most and give rise to a rounding of the upper part of the pulse transition. As the pulses become narrower, this rounding begins to reduce the steady-state level and limits the usefulness of the cables. The pulse response of the three types of cables was evaluated. A pulse-forming passive network (Picosecond Pulse Labs Model 5220X) was used in line with an oscilloscope source to launch an excitation 2 ns (500 Mb/s) wide. The propagated waveforms at the output are shown in Figure 8. The 0.254-mm (10-mil)-diameter ribbon cable exhibited both higher dc drop (reduction of amplitude) and rise-time dispersion because of the increased attenuation which rounds the upper part of the pulse. Table 1 lists the measured rise-time dispersion for 2-m lengths of the different cables and 50-cm-long flexiblefilm structure. The coaxial 25AWG cable transmitted the fastest signal, with an output rise time of 353 ps, while the ribbon cable was fairly dispersive. From the pulse distortion shown in Figure 8 it was concluded that the 50-cm-long flexible-film cable is equivalent in performance to a 2-m-long coaxial cable.

The test card traces were characterized with the shortpulse technique using lines 7.6 cm and 12.7 cm (3 and 5 in.) long. The measured attenuation was compared to calculated values based on the card dimensions obtained





Element

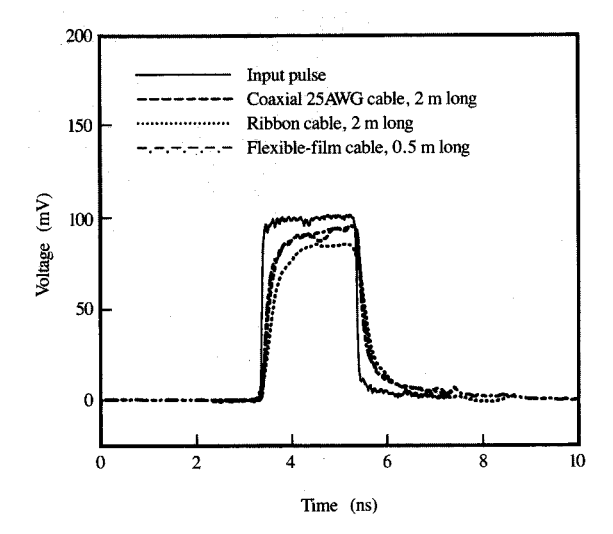
(a) Near-end noise and (b) far-end noise using 300-ps step source from card only (dashed lines) and from card with cable attached (solid lines). The results shown were obtained with the coaxial-cable 90° carrier.

and the vias and pads, without the cables attached. The test pads were on a 1.27-mm (50-mil) pitch. Crosstalk was monitored both at the end close to the excitation, for nearend noise, and at the end of the card trace, for far-end noise. The measurement was repeated with the cables attached, and the same points were monitored. The difference between the two results was considered to be the final crosstalk. Linear superposition was generally assumed, and a doubling was expected for the case of two active lines with one quiet line in the middle [6]. The measurement was actually carried out with only one active and one quiet line because of limitations in the experimental setup. Waveforms of the NEN and FEN components for the coaxial 90° carrier are shown in Figure 7. The card-only measurements (dashed traces) are shown as well. Table 2 summarizes the results obtained.

from cross-sectioning and the techniques explained in [6]. The frequency-dependent attenuation, phase constant, and characteristic impedance of the cables and card wiring were used as input to a circuit simulator program [7] to model the signal propagation for the 2-m coaxial 25AWG cable with a 25.4-cm length of test card trace (12.7 cm at either end) included in the path. Models for the capacitive and inductive discontinuities associated with the test pads and vias and the connector were also included. The good agreement shown in Figure 9 between the two waveforms confirmed the validity of the analysis because the amplitude of the reflections and the similarity of the waveforms depend directly on the connector characteristics and the frequency-dependent losses of the card and the cable lines.

Maximum useful cable length

The results of the previous sections were used to conduct a study of the maximum useful cable length for the various options of Table 1; cable length is the most relevant parameter for system applications. Pulse inputs with 1- and 2-ns widths and 1-V amplitude, transmitted at clock rates of 2 and 4 ns (1 Gb/s and 500 Mb/s), respectively, were assumed in the study. The signals had 300-ps rise and fall times. The criterion for usefulness was that the propagated signal had to achieve at least a 600-mV level when the path was terminated via a characteristic impedance of 50 Ω . The need for a 60% signal swing arriving at the receiver input was based on the assumption that the crosstalk was $\pm 10\%$, ΔI noise was $\pm 15\%$, and receiver switching threshold variation was ±5% around the midpoint of the swing, for the rising and falling signal transitions, respectively. This assumption allowed for additional signal degradation due to changes in electrical characteristics caused by processing tolerances, power supply variations, and operating temperature fluctuations. Representative paths were modeled with the electrical discontinuities due to the cable connectors and card vias, as well as the measured frequency-dependent losses of the signal lines in the test card and cables. The FR-4 (fire-retardant, epoxyglass cloth) dielectric of the card wiring was measured with the technique of [8] and shown to have a tan δ of 0.025, a loss which is considered quite high compared to that of other insulators used in packaging structures (ceramic, for example). It was explained in [6] and can be seen in Figure 5 that in the case of lines with small resistive losses such as the card traces, the dielectric loss dominates even at low frequencies. This is one reason why the attenuation for the card trace is so much higher than for the cable lines separated by a lossless insulator (PTFE). When large numbers of cables are required in a specific application, substantial lengths of card wiring are required to connect associated driver and receiver circuits to the cable. Then



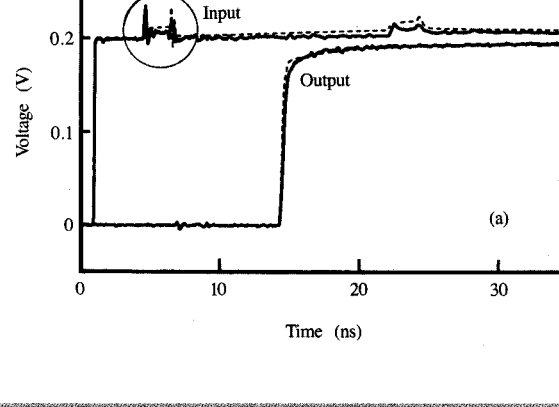
Response of cables to 2-ns-wide input pulses. The waveforms shown appeared at the end of each of the indicated cables. The solid line depicts the input excitation.

Table 3 Maximum useful cable length obtained from simulation.

Cables modeled	Cable + 2 card w	,	Cable only		
	@ 500 Mb/s	@ 1 Gb/s	@ 500 Mb/s	@ 1 Gb/s	
	(m)	(m)	(m)	(m)	
Coaxial 25AWG	3.5	1.5	5.25	3.0	
Ribbon	2.5	1.75	4.0	2.5	
Flexible-film	1.6	1.0	2.5	1.5	

losses in the card can dominate and limit the maximum useful cable length due to excessive rise-time dispersion.

Table 3 lists the simulation results obtained for the various cables for 500-Mb/s and 1-Gb/s data streams and for the cases with and without card or board losses. The coaxial 25AWG cable with an expanded PTFE insulator should be useful up to 5.25-m lengths at 500-Mb/s data rates. The length reduces to 3.0 m for 1-Gb/s transmission. In this case, the rise-time dispersion reduces the steady-state level because of rounding of the upper and lower parts of the rise and fall times of the pulses, as is explained in [9]. Skin-effect and dielectric losses in the card traces and distortions caused by the reflections from connectors and vias further slow down the rise time and reduce the expected useful lengths to 3.5 and 1.5 m at



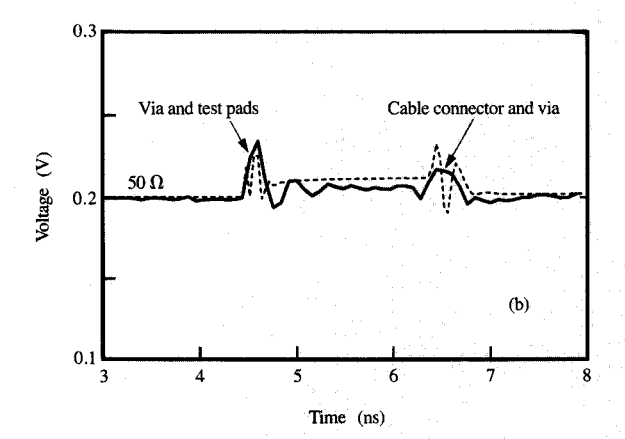


Figure 9.

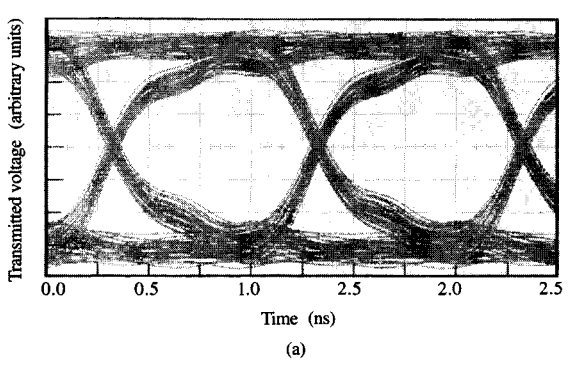
0.3

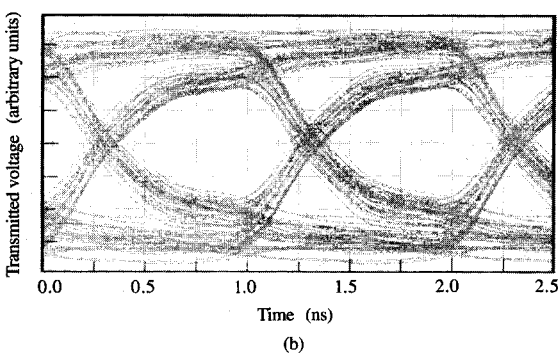
(a) Measured (solid line) and simulated (dashed line) input and output TDT response for 2-m-long coaxial 25AWG cable. (b) Behavior in circled region of (a) showing reflections from 12.7-cm-long test card wiring, card vias, and cable connector.

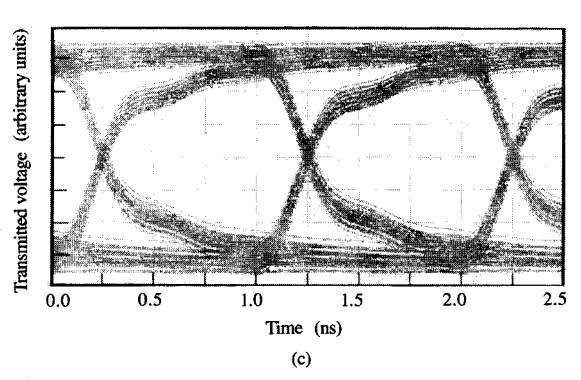
500-Mb/s and 1-Gb/s rates, respectively. In this case the same cable was attached to 20-cm-long card lines (10 cm at each end). As was seen in Figure 5, the ribbon cable displays a much larger attenuation and yields shorter useful lengths. The flexible-film cable, which offers the highest density, is expected to be useful only for 1.0-2.5-m lengths. It should be noted that in practical applications in which higher-density, narrower card wiring is used, the maximum useful cable length is expected to be substantially less.

The simulation results presented above were confirmed by bit-error rate (BER) and eye-closure measurements performed on the coaxial 25AWG, ribbon, and flexible-film cables. Such measurements are commonly used in optical fiber data transmission evaluations, but are also useful in analyzing the performance of electrical cables. A pseudorandom data pattern was created using the ANRITSU Pulse Pattern Generator MPI604A, and errors were counted using an ANRITSU Error Detector MP1605A. Data rates ranging from 200 Mb/s to 2.5 Gb/s were generated with a rise time of 100 ps. Measurements were performed by launching the data stream with coaxial probes both close to the cable ends (0.86-cm-long card wiring), or some distance away (12.7-cm-long card wiring at both ends) using the test cards shown in Figure 3. The random pattern generator simulated typical data streams found in digital data transmission. The transmitted signals were detected with an oscilloscope synchronized with the data generator. Figure 10 shows "eye diagram" data streams for the 2-m-long coaxial 25AWG cable, the 2-mlong ribbon cables, and the 50-cm-long flexible-film cable, at a 1-Gb/s data rate. As expected from the attenuation results of Figure 5, there is a more pronounced closing of the "eye" for the 2-m-long ribbon cable than for the 2-m-long coaxial cable. This is caused both by rise-time dispersion and by a larger dc drop. Rise-time dispersion is caused by frequency-dependent losses in the cable and by the reflections at the cable connectors. In addition, a variable data pattern exacerbates the signal distortion because each pulse has a variable starting steady-state level, depending on the number of consecutive low or high states (0s or 1s) in the data. This is especially true for pulses that are narrower than the round-trip delay on the signal path [10]. The pulse switches direction before the signal is able to reach the full steady-state level. A 40-50% loss of the "eye opening," or the area of the waveform, is associated with a reasonable signal at the receiver-circuit input to overcome all the anticipated noise sources discussed earlier. It was found that an adequate eye opening could be obtained with the 2-m-long coaxial 25AWG cable up to 1.6 Gb/s, while with the same length of ribbon cable, an adequate eye opening could be obtained only up to 1 Gb/s. For 3-m-long cables, the upper limits were 1.3 and 0.7 Gb/s, respectively. As can be seen from Figure 10(c), the 50-cm-long flexible-film cable displayed an adequate eye opening at 1 Gb/s, similar to the coaxial 25AWG cable, but for one quarter the cable length. The upper limit for the 50-cm flexible-film cable was 1.6 Gb/s.

The maximum data rates dropped further when the 25.4cm length of card wiring was incorporated into the circuit, because of the substantial additional loss that was thereby introduced. Figure 11 shows the corresponding results obtained for the 2-m-long coaxial 25AWG cable at 500-Mb/s, 1-Gb/s, and 1.6-Gb/s rates. The acceptable bitrate limit was found to drop from 1.6 Gb/s to 1.3 Gb/s. A comparison of the waveforms of Figures 10(a) and 11(b), both of which were obtained at a 1-Gb/s rate, highlights

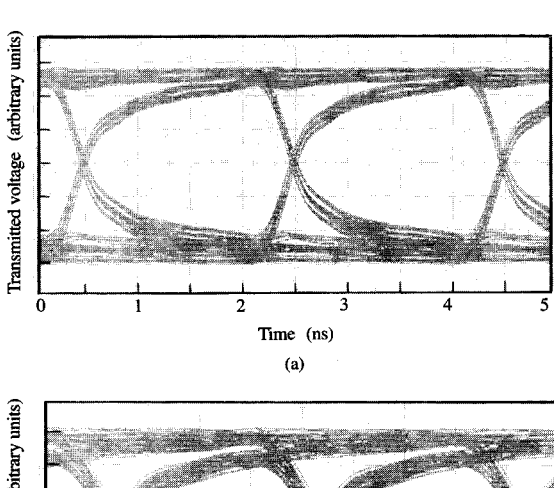


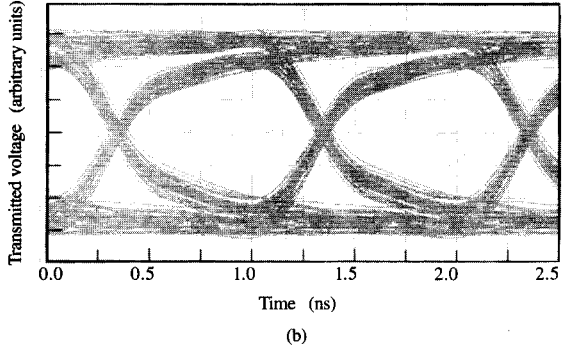


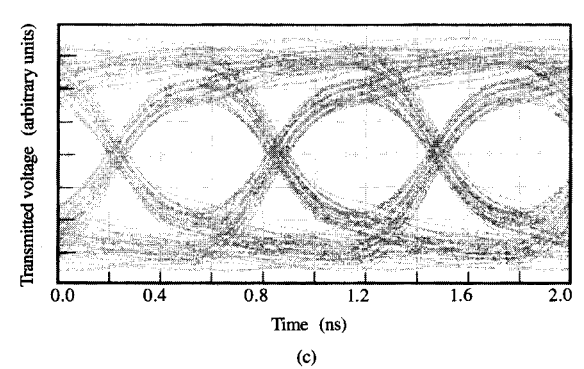


English (i

Eye diagrams obtained at 1-Gb/s data rate from (a) 2-m-long coaxial 25AWG cable, (b) 2-m-long ribbon cable, and (c) 0.5-m-long flexible-film cable. An 0.86-cm length of test card wiring was included at each end of the cables. Note that the quality of the eye diagrams is poor because of the statistical variation of the data patterns depicted in them.







Figure

Eye diagrams obtained with 2-m-long coaxial 25AWG cable, at (a) 500-Mb/s, (b) 1-Gb/s, and (c) 1.6-Gb/s data rates. The path traversed by the signal included two 12.7-cm lengths of card wiring and connectors at each end of the cable.

the effect of the card losses on signal integrity. In all cases, a BER lower than 10^{-12} was measured. Such a low error rate is considered adequate for most digital systems that have some type of built-in error detection and correction mechanism. Generally, passive electrical interconnections of the kind discussed in this paper contain no physical mechanisms that can introduce random failures. Signal degradation, however, has been shown to

limit their maximum useful lengths. The results are consistent with the predicted limits of Table 3.

Summary and discussion

In summary, we have presented a study of the relative performance and key limiting factors of coaxial, shieldedribbon, and flexible-film cables under consideration for use as intrasystem interconnections for 500-Mb/s-1-Gb/s data rate applications. It was found that coaxial cables with low-loss insulators offer the longest useful lengths (3-5.25 m). Thermoplastic elastomers introduce higher dielectric losses. A thick braided outer conductor was found to be much less lossy than thin foils for the shielding of coaxial cables. Signal conductors narrower than 0.457 mm (18 mils) were found to be unable to provide connections of very long length in the 1-Gb/s range. The design of the connector was found to be very important with regard to impedance matching and crosstalk. Individual shielded carriers were found to be superior to other types of connectors that fan out the cable to coarse pin arrangements at the card interface. Surface-mount connectors, such as those integrated with flexible-film cables, should ultimately offer the highest density and, in time, lowest cost. Much of the cost of all of the cables investigated was found to be in the assembly of their end connectors. Both the coaxial and ribbon cables cost about 50 cents per foot of length. A good coaxial connector, such as the 90° carrier and straight header discussed in this paper, can cost as much as \$7-10 per signal line. Even the ribbon-cable connector, which can be machine-assembled, still costs about \$1.2 per signal line. If one considers a 2-m-length application, a coaxial solution would cost \$10-13 per signal, while a ribbon cable would require \$4.4 per line. A batch-fabricated flexible-film cable, with the connector being part of the photolithographic fabrication sequence, would offer lower cost.

Well-engineered cable connectors contain fully shielded signal conductors inside the cable carrier and card header, and connect to the card with one ground and one signal pin per cable. Other configurations, in which the connector itself might be quite dense but then fans out to four to six rows of pins in the card, result in increased crosstalk and large discontinuities, as well as a reduction of density. The density in both cases is dictated primarily by the diameter (greater than 0.254 mm) of the signal wire in the cable needed to retain low resistive losses over long lengths. Also, any pinned connector is limited in density, since printed-circuit boards cannot be fabricated with throughvia holes on grids smaller than 1.27 mm (0.05 in.). Ribbon cables offer the potential for high density, but the requirement of use over several meters necessitates large conductor cross sections, limiting their potential for miniaturization. Stacking may be used with most cables at the cost of increased connector complexity. Thin, flexiblefilm cables can easily be stacked in multiple strips that require substantially less space than ribbon cables and (especially) coaxial cables. Furthermore, flexible-film cables require surface-mount attachment to the cards, resulting in smaller electrical discontinuities at the interface. This permits higher wiring density in the cards because wiring channels are not thereby blocked by pins. Currently, card technology limits the surface pads to grids of 0.635-1.27 mm (0.025-0.05 in.) because of processing tolerances. Photolithographically fabricated high-density cards should improve top surface connectivity. The conductor density of a flexible-film cable is limited by the via dimensions at its end pads, which continue to require the use of 0.635-1.27-mm (0.025-0.05-in.) grids. While punching or mechanical drilling is used currently to create the vias, laser drilling can reduce the grid size substantially, but at much higher cost. The use of smaller vias permits the use of several rows of signal contacts, leading to a higher connector density. While thick layers can be laminated together, small vias cannot be fabricated in the resulting structure, and its stiffness becomes unmanageable. As discussed in [9], conductor cross sections larger than 0.203×0.035 mm (8 \times 1.4 mils) are not considered feasible, thus limiting useful lengths of flexible-film cables to less than 2.5 m.

In a specific system application, many factors must be considered in order to determine the maximum useful lengths of different cable options. These include the physical location of the driver and receiver circuits; noise budgets; the losses in the printed-circuit-board signal lines; the impedance mismatches between the cards, cables, connectors, and terminating resistors; the inductive and capacitive discontinuities due to the connectors and vias; crosstalk; and the tolerances of all these components. Electrical intrasystem interconnections can offer viable solutions for most applications. As system integration at the chip, chip carrier, and printed-circuit-board level continues to increase, the lengths of the cables required should decrease. At the same time, however, data rates will increase, and throughput might reach a limit not overcome by serialization or the widening of data bases. At that point, optical interconnections may become more favorable because of their higher speed and better electromagnetic control, despite their higher cost.

PS/2 is a registered trademark of International Business Machines Corporation.

Teflon and Kapton are registered trademarks of E. I. du Pont de Nemours & Co.

References

 R. E. Matick, Transmission Lines for Digital and Communication Networks, McGraw-Hill Book Co., Inc., New York, 1969.

- V. A. Ranieri, A. Deutsch, G. V. Kopcsay, and G. Arjavalingam, "A Novel 24-GHz Bandwidth Coaxial Probe," *IEEE Trans. Instr. & Meas.* 39, 504-507 (1990).
- 3. A. Deutsch, G. Arjavalingam, and G. V. Kopcsay, "Characterization of Resistive Transmission Lines by Short-Pulse Propagation," *IEEE Microwave & Guided Wave Lett.* 2, 25-27 (1992).
- B. Beaman, D. Y. Shih, and G. Walker, "A New Direction for Elastomeric Connectors," Proceedings of the 43rd Electronic Components and Technology Conference, ECTC '93, IEEE/EIA, 1993, pp. 463-467.
- M. A. Steele, "Horizons for Flexible Circuits," Interconnection Technol. 2, 27-29 (1993).
- A. Deutsch, G. V. Kopcsay, V. A. Ranieri, J. K. Cataldo, E. A. Galligan, W. S. Graham, R. P. McGouey, S. L. Nunes, J. R. Paraszczak, J. J. Ritsko, R. J. Serino, D. Y. Shih, and J. S. Wilczynski, "High-Speed Signal Propagation on Lossy Transmission Lines," *IBM J. Res.* Develop. 34, 601-615 (1990).
- Advanced Statistical Analysis Program (ASTAP), Program Reference Manual, Order No. SH20-1118-0; available through IBM branch offices.
- G. Arjavalingam, Y. Pastol, J.-M. Halbout, and G. V. Kopcsay, "Broadband Microwave Measurements with Transient Radiation from Optoelectronically Pulsed Antennas," *IEEE Trans. Microwave Theory Technol.* MTT-38, 615-621 (1990).
- A. Deutsch, D. W. Dranchak, G. Arjavalingam, C. W. Surovic, J. K. Tam, G. V. Kopcsay, and J. B. Gillett, "Electrical Characterization and Performance Limits of a Flexible Cable," *IBM J. Res. Develop.* 37, 22-38 (1993).
- A. Deutsch and C. W. Ho, "Triplate Structure Design for Thin Film Lossy, Unterminated Lines," Proceedings of the 1981 IEEE International Symposium on Circuits and Systems, IEEE, 1981, pp. 1-5.

Received January 21, 1994; accepted for publication June 29, 1994

Alina Deutsch IBM Research Division, Thomas J. Watson Research Center, P.O. Box 218, Yorktown Heights, New York 10598 (deutsch@watson.ibm.com). Mrs. Deutsch received B.S. and M.S. degrees in electrical engineering from Columbia University and Syracuse University, respectively; she has worked at IBM since 1971. She is a Senior Engineer, currently working on the design, analysis, and measurement of packaging structures for future digital processor and communication applications. Mrs. Deutsch is an author or coauthor of a number of technical papers and a co-inventor of seven U.S. patents. She received an IBM Outstanding Technical Achievement Award in 1990 and an IBM Research Division Award in 1993. She is a member of Tau Beta Pi and Eta Kappa Nu, and a senior member of the IEEE.

G. Arjavalingam Needham and Company, 400 Park Avenue, New York, New York 10022. Dr. Arjavalingam obtained a B.A. degree from Cambridge University, U.K., in 1978, and M.S. and Ph.D. degrees from the University of California at Berkeley in 1980 and 1983, respectively, all in electrical engineering. From July 1983 to January 1994 he was at the Thomas J. Watson Research Center, where he worked on the production and various applications of ultrashort pulses. In January 1994, he received an IBM Outstanding Technical Achievement Award for his work on the use of ultrashort electromagnetic transients for broad-band microwave measurements. From October 1989 to January 1994, he managed the Package Design, Analysis, and Measurements group. He is currently an Equities Analyst at Needham and Company, Investment Bankers, responsible for covering communications technology. Dr. Arjavalingam is a senior member of the IEEE and a member of the Optical Society of America.

Christopher W. Surovic IBM Research Division, Thomas J. Watson Research Center, P.O. Box 218, Yorktown Heights, New York 10598 (CWS at YKTVMV). Mr. Surovic is pursuing his associate degree in mechanical science and engineering at Westchester Community College. He has been at IBM since 1989. He worked in the area of tool and model making for about four years and made contributions to the development of laser ablation tools and the Smithsonian X-ray Telescope. Mr. Surovic is currently a laboratory technician, working on electrical characterization of package structures for future computer applications. He is a coauthor of several papers on electronic packaging measurements.

Alphonso P. Lanzetta IBM Research Division, Thomas J. Watson Research Center, P.O. Box 218, Yorktown Heights, New York 10598 (PTLANZ at YKTVMV).

Keith E. Fogel IBM Research Division, Thomas J. Watson Research Center, P.O. Box 218, Yorktown Heights, New York 10598 (FOGEL at YKTVMV). Mr. Fogel received a B.S. degree in electrical engineering from Fairleigh Dickinson University and has been at IBM since 1988. He is a Senior Associate Engineer, currently working on a technique for temporary chip attachment at the wafer level and on elevated-temperature chip testing. He is a co-inventor of four U.S. patents, and received an IBM Outstanding Technical Achievement Award in 1993 and an IBM Research Division Award in 1994.

Fuad Doany IBM Research Division, Thomas J. Watson Research Center, P.O. Box 218, Yorktown Heights, New York 10598 (DOANY at YKTVMV). Dr. Doany received a B.S. degree in chemistry from Haverford College in 1978 and a Ph.D. degree in physical chemistry from the University of Pennsylvania in 1984. From 1984 to 1985 he carried out postdoctoral studies in chemical physics at the California Institute of Technology. He joined the IBM Research Division in 1985 and is currently a Research Staff Member in the Optical Systems group at the Thomas J. Watson Research Center. Dr. Doany's work at IBM has focused on laser spectroscopy, laser material processing, and optical engineering. He is an author or coauthor of a number of technical papers and the co-inventor of seven U.S. patents. Dr. Doany received an IBM Research Division Award in 1994. He is a member of the Optical Society of America.

Mark B. Ritter IBM Research Division, Thomas J. Watson Research Center, P.O. Box 218, Yorktown Heights, New York 10598 (ritter@watson.ibm.com). Dr. Ritter received a Ph.D. degree in applied physics from Yale University in 1987. He is a Research Staff Member, working on fiber-optic data communication links, high-throughput parallel optical buses, and wireless data communication links and networks. Dr. Ritter was the recipient of the 1982 American Physical Society Apker Award. He is an author or coauthor of more than 17 papers and a co-inventor of eight U.S. patents.